NeuroImage: Clinical 8 (2015) 51–58

Contents lists available at ScienceDirect

NeuroImage: Clinical

journal homepage: www.elsevier.com/locate/ynicl

Tract shape modeling detects changes associated with preterm birth and neuroprotective treatment effects

Devasuda Anblagan[a,b], Mark E. Bastin[b], Sarah Sparrow[a], Chinthika Piyasena[c], Rozalia Pataky[a], Emma J. Moore[a], Ahmed Serag[a], Alastair Graham Wilkinson[d], Jonathan D. Clayden[e], Scott I. Semple[f], James P. Boardman[a,b,*]

[a]MRC Centre for Reproductive Health, University of Edinburgh, 47 Little France Crescent, Edinburgh EH16 4TJ, UK
[b]Centre for Clinical Brain Sciences, University of Edinburgh, Chancellor's Building, 49 Little France Crescent, Edinburgh EH16 4SB, UK
[c]Centre for Cardiovascular Science, University of Edinburgh, 47 Little France Crescent, Edinburgh EH16 4TJ, UK
[d]Department of Radiology, Royal Hospital for Sick Children, 9 Sciennes Road, Edinburgh EH9 1LF, UK
[e]Institute of Child Health, University College London, 30 Guilford Street, London WC1N 1EH, UK
[f]Clinical Research Imaging Centre, University of Edinburgh, 47 Little France Crescent, Edinburgh EH16 4TJ, UK

ARTICLE INFO

Article history:
Received 19 February 2015
Received in revised form 17 March 2015
Accepted 26 March 2015
Available online 28 March 2015

Keywords:
Preterm
Infant
Magnetic resonance image
Brain
Neuroprotection
Magnesium sulfate

ABSTRACT

Preterm birth is associated with altered connectivity of neural circuits. We developed a tract segmentation method that provides measures of tract shape and integrity (probabilistic neighborhood tractography, PNT) from diffusion MRI (dMRI) data to test the hypotheses: 1) preterm birth is associated with alterations in tract topology (R), and tract-averaged mean diffusivity (⟨D⟩) and fractional anisotropy (FA); 2) neural systems are separable based on tract-averaged dMRI parameters; and 3) PNT can detect neuroprotective treatment effects.

dMRI data were collected from 87 preterm infants (mean gestational age 29^{+1} weeks, range 23^{+2}–34^{+6}) at term equivalent age and 24 controls (mean gestational age 39^{+6} weeks). PNT was used to segment eight major fasciculi, characterize topology, and extract tract-averaged ⟨D⟩ and FA.

Tract topology was altered by preterm birth in all tracts except the splenium ($p < 0.05$, false discovery rate [FDR] corrected). After adjustment for age at scan, tract-averaged ⟨D⟩ was increased in the genu and splenium, right corticospinal tract (CST) and the left and right inferior longitudinal fasciculi (ILF) in preterm infants compared with controls ($p < 0.05$, FDR), while tract-averaged FA was decreased in the splenium and left ILF ($p < 0.05$, FDR). Specific fasciculi were separable based on tract-averaged ⟨D⟩ and FA values. There was a modest decrease in tract-averaged ⟨D⟩ in the splenium of preterm infants who had been exposed to antenatal $MgSO_4$ for neuroprotection ($p = 0.002$).

Tract topology is a biomarker of preterm brain injury. The data provide proof of concept that tract-averaged dMRI parameters have utility for evaluating tissue effects of perinatal neuroprotective strategies.

1. Introduction

Globally, preterm birth (defined as birth at <37 weeks of gestation) affects around 11% of deliveries (Blencowe et al., 2013) and it is closely associated with cerebral palsy, cognitive impairment and neuropsychiatric disease in later life (Kerr-Wilson et al., 2012; Moore et al., 2012). Individuals born preterm are more likely to experience behavioral and emotional disturbance (Clark et al., 2008; Elgen et al., 2012), autistic spectrum disorder (Johnson et al., 2010), attention deficit hyperactivity disorder (Bhutta et al., 2002) and psychiatric disease, and these problems persist into adulthood (Crump et al., 2010; Halmoy et al., 2012; Moster et al., 2008; Nosarti et al., 2012).

White matter disease is a core feature of the encephalopathy of prematurity and it is associated with reduced connectivity of neural circuitry (Ball et al., 2013; Boardman et al., 2006; Fischi-Gomez et al., 2014; Pandit et al., 2014; Woodward et al., 2006). Antenatal magnesium sulfate ($MgSO_4$) is often given to women expected to deliver preterm because it is associated with reduced rates of cerebral palsy (Doyle et al., 2007). However, there are uncertainties about its long-term effects, and studies have not been designed or powered to investigate its influence on non-motor functions (Chollat et al., 2014; Doyle et al., 2014). Biomarkers of tissue integrity in the tracts of neural systems that subserve a range of functions are required to evaluate more pervasive neuroprotective effects.

Diffusion MRI (dMRI) and tractography enable measures of white matter tract integrity to be determined in specific tracts-of-interest

* Corresponding author at: Room W1.26, MRC, University of Edinburgh, Centre for Reproductive Health, Queen's Medical Research Institute, 47 Little France Crescent, Edinburgh EH16 4TJ, UK. Tel.: +44 131 242 2567; fax: +44 131 242 6441.
E-mail address: james.boardman@ed.ac.uk (J.P. Boardman).

http://dx.doi.org/10.1016/j.nicl.2015.03.021

(TOIs) (Basser et al., 2000). Tractography techniques use deterministic (Conturo et al., 1999) or probabilistic (Behrens et al., 2007) approaches to identify the major pathways, with tracts initiated at seed points and typically constrained by operator-defined 'waypoints' through which streamlines must pass or stop. Segmented pathways can then be analyzed as 3-dimensional regions-of-interest and water molecule diffusion parameters extracted. Neonatal dMRI data present challenges to tractography algorithms because of smaller head size, resolution difficulties, wide anatomic variation, increased brain water content, and lack of reference atlas data from typically developing newborns. Consequently, neonatal studies have tended to focus on a relatively small number of TOIs, none has provided information about tract topology, and few have included control data.

An alternative technique for segmenting TOIs is provided by probabilistic neighborhood tractography (PNT). In this method, single seed point tractography is used to segment the same TOI across a group of subjects by modeling how individual tracts compare with a predefined reference in terms of length and shape (Bastin et al., 2010; Clayden et al., 2006; Clayden et al., 2007). To achieve this, candidate seed points are automatically placed in a cubic neighborhood of native space voxels, with the tract that best matches the reference tract chosen as its representation in each subject (Bastin et al., 2010; Clayden et al., 2006; Clayden et al., 2007). The output includes tract-averaged water diffusion tensor parameters, mean diffusivity (⟨D⟩) and fractional anisotropy (FA), and the goodness-of-fit of the best-matched tract to the reference (R). The approach has been useful for mapping white matter change in normal development (Clayden et al., 2012), ageing (Bastin et al., 2010; Penke et al., 2010), and amyotrophic lateral sclerosis (Bastin et al., 2013). PNT overcomes the bias inherent to user-defined waypoint placement, does not require thresholding of connectivity values, and is unique in providing information about tract topology.

In this paper, we generated an atlas of reference tracts for eight TOIs using PNT to test the hypotheses that: 1) tract topology, and tract-averaged ⟨D⟩ and FA, are altered by preterm birth; 2) TOIs are separable in the newborn brain based on water diffusion parameters; and 3) PNT is sensitive to detecting perinatal neuroprotective treatment effects.

2. Methods and materials

2.1. Participants

Ethical approval was obtained from the National Research Ethics Service (South East Scotland Research Ethics Committee), and informed written parental consent was obtained. Preterm infants were recruited from the Royal Infirmary of Edinburgh between July 2012 and September 2014. Infants were eligible if they had a birth weight <1500 g and/or were born at <31 completed weeks' postmenstrual age (PMA). Exclusion criteria for the study were infants with congenital infection, major chromosomal abnormalities, cystic periventricular leucomalacia, post-hemorrhagic ventricular dilatation and porencephalic cysts. Healthy term-born control infants were recruited from antenatal clinics and postnatal wards.

MRI data from 24 healthy infants born at full term and 87 preterm infants (mean PMA at birth 29^{+1} weeks, range 23^{+2}–34^{+6} weeks) were acquired at term equivalent age (mean PMA 39^{+6} weeks, range 37^{+5}–42^{+5} weeks) (Table 1). Infants were examined in natural sleep with pulse oximetry, temperature and electrocardiography data monitoring. Ear protection was used for each infant, comprising earplugs placed in the external ear and neonatal earmuffs (MiniMuffs, Natus Medical Inc., CA).

2.2. MR image acquisition

A Siemens Magnetom Verio 3 T MRI clinical scanner (Siemens AG, Healthcare Sector, Erlangen, Germany) and 12-channel phased-array head coil were used to acquire: T1-weighted MPRAGE volume (~1 mm^3 resolution), T2-weighted STIR (~0.9 mm^3 resolution), T2-weighted FLAIR (~1 mm^3 resolution), and dMRI (11 T2- and 64 diffusion encoding direction ($b = 750$ s/mm^2) single-shot spin-echo echo planar imaging (EPI) volumes with 2 mm isotropic voxels) data.

2.3. Image analysis

dMRI data were pre-processed using FSL tools (FMRIB, Oxford, UK; http://www.fmrib.ox.ac.uk). This included brain extraction, and removal of bulk infant motion and eddy current induced artifacts by registering the diffusion-weighted to the first T2-weighted EPI volume for each subject. Using DTIFIT, ⟨D⟩ and FA volumes were generated for every subject. BedpostX/ProbTrackX algorithm was run with its default parameters: 2-fiber model per voxel, 5000 probabilistic streamlines for each tract with a fixed separation distance of 0.5 mm between successive points to generate the underlying white matter connectivity data (Behrens et al., 2003, 2007).

2.4. Reference tracts and model training data

Eight reference TOIs were created using PNT in standard space from the tractography output produced from a training set of 20 term controls: genu and splenium of corpus callosum, left and right projections of the corticospinal tract (CST), cingulum cingulate gyri (CCG) and inferior longitudinal fasciculi (ILF). Briefly, a set of 'candidate' tracts were generated by seeding within a $7 \times 7 \times 7$ neighborhood of native space voxels centered around a standard space seed point located within the center of the white matter structure-of-interest and transferred to the native space of each control. These standard space seed points were defined using an age specific T2-weighted neonatal template (http://www.brain-development.org) (Kuklisova-Murgasova et al., 2011). Then, an experienced observer (DA) selected candidate tracts from each control subject that best matched the anatomical shape of the white matter structure-of-interest. Using these visually-assessed 'best-matching' tracts, tract shape models were fitted to the tractography data using maximum likelihood (Clayden et al., 2007), thereby capturing the shape and length variation amongst the controls' tracts. Once the reference tracts and shape models had been created, PNT was re-run over a neighborhood of $3 \times 3 \times 3$ voxels centered on the reference tract and transferred to native space for all participants; the seed point that produced the best matching tract to the reference was then determined. All the computational analysis was implemented in TractoR (http://www.tractor-mri.org.uk) (Clayden et al., 2011).

2.5. Tractography analysis

Two experienced raters (DA, MEB) visually assessed the best-matched tracts. Any subject with deviated, aberrant or truncated pathways that were not anatomically plausible representations of the TOI were excluded from further analysis (Table 2). The tractography masks of the best match tracts were applied to the ⟨D⟩ and FA volumes, which permitted tract-averaged values of these biomarkers to be determined for each TOI in every subject. Finally, the goodness-of-fit of the best match tract to the reference (R) was determined from the log-ratio between the matching likelihood of the chosen candidate tract and the matching likelihood of the reference tract under the model. The more negative the R value, the less good the fit between the reference and best match tract.

2.6. Volumes of lateral ventricular system

The lateral ventricles were segmented in 59 out of 101 subjects for whom high resolution T1w and T2w structural data were available (10 controls and 49 preterms). An atlas-based image segmentation approach was used that included lateral ventricles and choroid plexus, but excluded the third and fourth ventricle, cavum septum pellucidum and

Table 1
Demographic information for the participants.

	Preterm at term equivalent age ($n = 79$)	Controls ($n = 22$)
PMA birth/weeks (mean and range)	29^{+1} (23^{+2} –34^{+6})	39^{+6} (38^{+1}–41^{+5})
Birth weight/kg (mean and range)	1.16 (0.550–1.635)	3.550 (2.870–4.670)
PMA at image acquisition/weeks (mean and range)*	40 (37^{+5}–42^{+5})	42 (39.0–45^{+3})
Weight at image acquisition (mean and range)*	2.890 (2.060–3.920)	3.628 (2.870–4.500)
Orbitofrontal head circumference at image acquisition (mean and range)*	34.7 (31.0–38.0)	36.1 (32.6–39.0)
Gender/M:F	41:38	10:12
Complete course of antenatal steroids[a]	57 (72%)	0
Antenatal $MgSO_4$ for fetal neuroprotection	40 (51%)	0
Bronchopulmonary dysplasia[b]	22 (28%)	n/a

* Indicates a statistically significant difference between groups ($p \leq 0.01$).
[a] Defined as first dose dexamethasone >24 h before birth.
[b] Defined as need for supplemental oxygen and/or respiratory support at 36 weeks' PMA.

vergae (Serag et al., 2012). This was done so that lateral ventricular size could be added as a co-variate to account for possible partial volume effects in the model testing independent effects of antenatal $MgSO_4$ on dMRI parameters, and to investigate correlation between *R* and ventricular size.

2.7. Statistical analysis

The distributions of ⟨D⟩, FA and *R* in each tract were assessed for normality using the Shapiro–Wilk test. The Mann–Whitney *U* test was used to compare *R* values between groups; Spearman's rho was used to investigate correlations between *R* and PMA at scan. Because age at scan differed between the two cohorts, and water diffusion parameters are dynamic over this developmental period, GLM univariate ANOVA was used to investigate the effect of prematurity on these biomarkers in each TOI with gestational age as a fixed factor and PMA at scan as a co-variate. Type 1 error was controlled using false discovery rate (FDR) ($p < 0.05$).

To investigate the effect of antenatal $MgSO_4$ exposure on tract-averaged ⟨D⟩ and FA, and *R*, independent of potential confounders, we first examined the association between these biomarkers with the following factors: exposure to a complete course of antenatal steroids, exposure to antenatal $MgSO_4$, gender and the presence of bronchopulmonary dysplasia (BPD). Significant factors in the bivariate analysis ($p < 0.05$) were included in a multivariate linear regression model that included PMA at birth. SPSS 21.0 (SPSS Inc., Chicago, USA) was used for analysis.

3. Results

3.1. Participants

FA volumes were blurred in eight preterm infants and two controls due to motion; these subjects were removed from further analysis leaving 79 preterm and 22 control infants in the analysis sample (demographic shown in Table 1). Two preterm infants required laser treatment for retinopathy of prematurity and 1 had a grade 3 intraventricular hemorrhage (IVH) identified on cranial ultrasound.

3.2. Segmentation of tracts-of-interest

Fig. 1 displays the reference TOIs that were identified reliably in the control training set in standard space. Across both preterm and control subjects, visual assessment of the individual segmented tracts indicated that PNT provided anatomically acceptable representations of the TOI for the vast majority of tracts (Table 2); for the preterm cohort this ranged from 100% (79/79) for CST to 82% (65/79) for right CCG.

3.3. Effect of preterm birth on tract topology

The distribution of *R* was negatively skewed for all TOIs. There was a significant difference in *R* between groups, with the preterm cohort having larger negative values, and hence greater topological difference from the reference compared to controls for all TOIs except the splenium (Table 3). Fig. 2 illustrates the range of values for *R* observed in the preterm cohort and how they correspond to tract shape for genu. There were no significant correlations between age at scan and *R*, with the exception of left CST. *R* correlated with ventricular volume for left ILF ($p = 0.009$) and left CST ($p = 0.004$), but not with any other TOI.

3.4. Effect of preterm birth on tract-averaged dMRI parameters

Table 2 shows tract-averaged water diffusion parameter values for each TOI for all participants. In bivariate analysis, tract-averaged ⟨D⟩ was higher in all tracts in preterm infants at term equivalent age compared with term controls, while FA was lower in all tracts except the right CCG. After adjusting for PMA at scan, tract-averaged ⟨D⟩ was increased in preterm infants at term equivalent age compared with controls in genu ($F = 17.57$, $p < 0.001$), splenium ($F = 19.22$, $p < 0.001$), left ILF ($F = 8.92$, $p = 0.004$) and right ILF ($F = 8.36$, $p = 0.005$).

Table 2
Mean (SD) for tract-averaged mean diffusivity (⟨D⟩) and fractional anisotropy (FA) for eight tracts-of-interest.

	Acceptable tracts		Mean diffusivity D ($\times 10^{-3}$ mm^2/s)				FA			
	Preterm ($n = 79$)	Control ($n = 22$)	Preterm	Control	Unadjusted *p*-value	Adjusted *p*-value*	Preterm	Control	Unadjusted *p*-value	Adjusted *p*-value*
Genu	74	22	**1.498 (0.080)**	**1.362 (0.068)**	<**0.001**	<**0.001**	0.21 (0.04)	0.25 (0.04)	<0.001	0.428
Splenium	68	22	**1.570 (0.152)**	**1.363 (0.067)**	<**0.001**	<**0.001**	**0.26 (0.04)**	**0.31 (0.04)**	<**0.001**	**0.009**
Left CCG	71	18	1.372 (0.095)	1.298 (0.044)	0.002	0.115	0.20 (0.03)	0.23 (0.03)	<0.002	0.738
Right CCG	65	18	1.350 (0.062)	1.286 (0.053)	<0.001	0.053	0.19 (0.03)	0.20 (0.02)	0.15	0.259
Left CST	79	21	1.227 (0.067)	1.157 (0.062)	<0.001	0.292	0.29 (0.03)	0.32 (0.02)	<0.001	0.147
Right CST	79	21	**1.178 (0.064)**	**1.107 (0.049)**	<**0.001**	**0.03**	0.27 (0.03)	0.30 (0.02)	0.001	0.469
Left ILF	76	19	**1.654 (0.237)**	**1.409 (0.071)**	<**0.001**	**0.004**	**0.20 (0.03)**	**0.23 (0.02)**	<**0.001**	**0.01**
Right ILF	78	21	**1.710 (0.254)**	**1.503 (0.163)**	**0.001**	**0.005**	0.22 (0.03)	0.24 (0.02)	0.003	0.134

* Adjusted *p*-values are corrected for postmenstrual age at scan and bold type indicates significant differences in tract-averaged values after adjustment (significance threshold $p < 0.05$, FDR corrected)

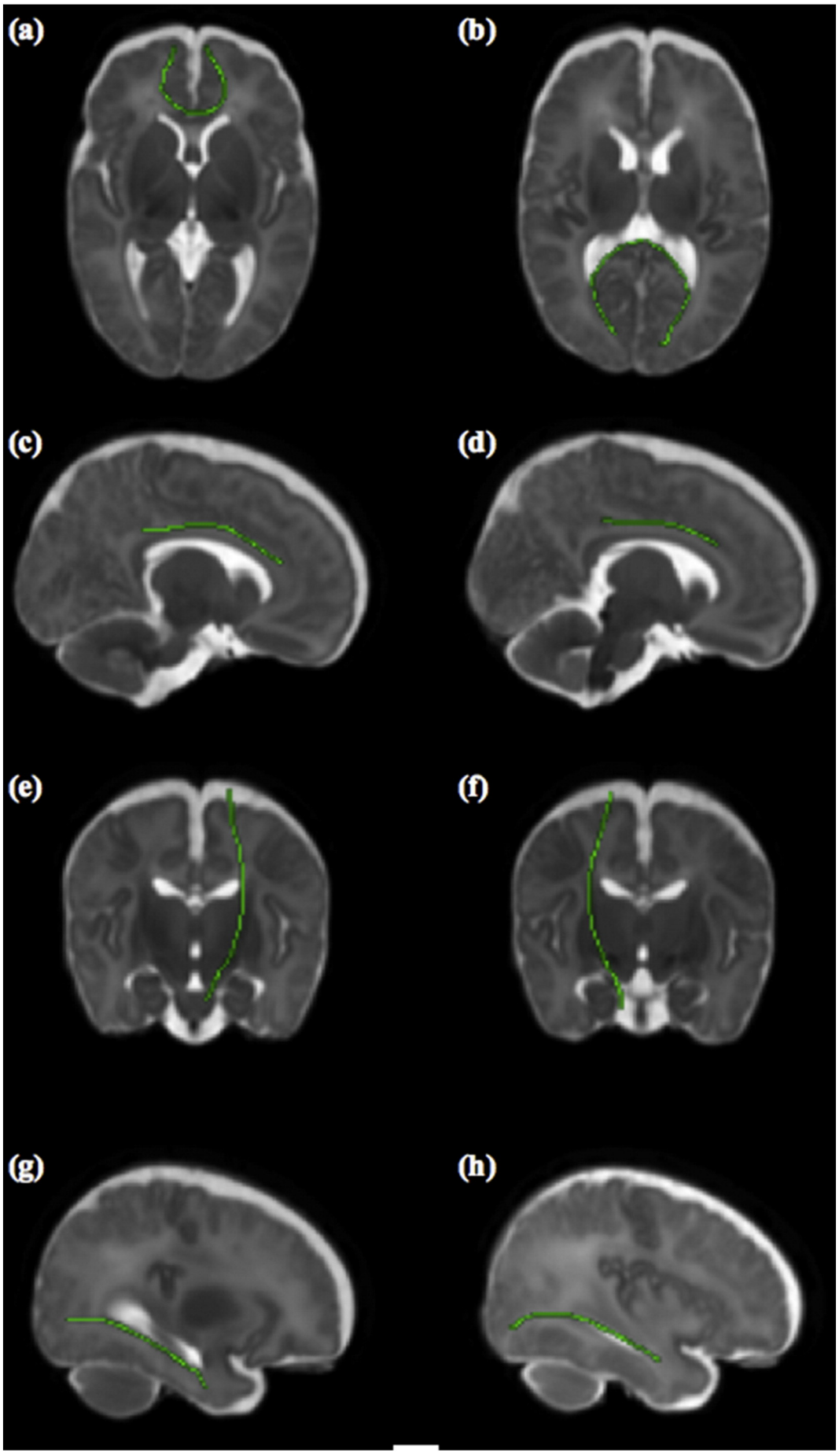
(a)
(b)
(c)
(d)
(e)
(f)
(g)
(h)

Table 3
Median (IQR/2) values of *R* for each tract. Significance testing carried out using Mann–Whitney *U* test. Bold type indicates significant differences in *R* ($p < 0.05$, FDR corrected).

	R		
	Preterm at term equivalent age	Control	*p*-Value
Genu	**−2.67 (2.08)**	**−1.44 (1.68)**	**0.017**
Splenium	−5.42 (3.16)	−3.08 (4.62)	0.108
Left CCG	**−1.88 (2.56)**	**0.57 (1.07)**	**0.001**
Right CCG	**−1.18 (2.11)**	**0.03 (1.52)**	**0.034**
Left CST	**−2.49 (1.22)**	**−0.63 (0.71)**	**<0.001**
Right CST	**−2.10 (1.14)**	**−0.97 (1.06)**	**0.006**
Left ILF	**−0.28 (1.48)**	**0.83 (1.23)**	**0.016**
Right ILF	**−2.26 (2.21)**	**−1.03 (1.88)**	**0.023**

Tract-averaged FA was reduced in the splenium ($F = 7.16$, $p = 0.009$) and left ILF ($F = 6.73$, $p = 0.01$) in preterm infants compared with controls after adjustment for age at scan.

3.5. Major fasciculi are separable in the newborn period based on dMRI parameters

Fig. 3 displays a scatterplot of tract-averaged ⟨D⟩ versus FA values for the eight TOIs. This figure indicates that CST, CCG, splenium and, to a lesser extent, ILF and genu are separable.

3.6. Effect of antenatal $MgSO_4$ exposure on water diffusion parameters in the major fasciculi at term equivalent age

Forty (51%) of the preterm cohort had been exposed to antenatal $MgSO_4$, and this was associated with lower ⟨D⟩ in splenium (mean difference −0.089 mm^2/s, 95% CI −0.161 to −0.017, $p = 0.016$).

In multivariate analysis, antenatal $MgSO_4$ was associated with a modest but significant decrease in ⟨D⟩ in splenium independent of age at birth and BPD (beta 115.0, 95% CI 43.4–186.5, $p = 0.002$). Factors included in the model were: PMA at birth because there was a difference between those who had [mean PMA 28^{+4} weeks] and had not been exposed to antenatal $MgSO_4$ [mean 29^{+6} weeks]; and BPD, because it influenced FA on univariate analysis (mean difference −0.03, 95% CI −0.05 to −0.005, $p = 0.015$). There was no effect of PMA at scan, which did not differ between the two groups (mean 39^{+6} weeks versus mean 40 weeks), or gender in univariate analysis, so these variables were not included.

Ventricular volumes were available for a subset of 28 of the treated group and 21 of the untreated group. There was no significant difference in ventricular volume between treated and untreated infants (8.4 versus 9.8 cm^3, $p = 0.11$), and in a subset analysis of infants where ventricular volume was entered into the model, antenatal $MgSO_4$ exposure retained significance (beta 100.1, 95% CI 28.8–172.3, $p = 0.007$). These data suggest that the observed difference in ⟨D⟩ is unlikely to be attributable to the partial volume effects from CSF.

4. Discussion

We developed a single seed point tractography-based segmentation algorithm (PNT) that incorporates tract shape modeling for use in neonates, and have segmented reliably eight major fasciculi. The algorithm is unique in providing a metric of tract topology, *R*, which measures the goodness-of-fit of the best matched tract with respect to an age specific tract template, and enables the extraction of tract-averaged water diffusion parameters including ⟨D⟩ and FA.

The advantages of PNT over region-of-interest and voxel-based methods for group-wise comparisons of ⟨D⟩ and FA are that it avoids the need for waypoint placement and setting of connectivity thresholds, and tracts are segmented in native space, which minimizes operator bias and takes account of individual differences in white matter structure. The method uses connectivity data produced by a probabilistic tractography algorithm, FSL's BedpostX/ProbTrackX, that can model multiple fiber populations and track through regions of reduced anisotropy, which has particular utility in neonates. Furthermore, by modeling the tracts of the whole study group with respect to reference tracts generated from an age specific training set, it is possible to perform group-wise analyses to study perinatal influences on *R*, and tract-averaged ⟨D⟩ and FA.

The measurement *R*, which indicates how the length and shape of the best-matched tract in each subject differs from reference tract topology, was significantly altered in preterm infants at term equivalent age compared with term controls in all tracts except splenium. To our knowledge this is the first evaluation of tract topology differences in a neonatal cohort. Our data suggest that tract shape change occurs independently of ⟨D⟩ and FA, and is less influenced by age at scan than these measures. Therefore, *R* may add value beyond other biomarkers that are affected by age at scan, which can be challenging to standardize in neonatal studies. A measure of tract shape is also particularly relevant given the wide anatomic variability of the brain at this stage of life, which is not captured in most tractography models. Further work is required to understand the functional correlates of *R* and whether it alters over time, but longitudinal studies of preterm infants suggest that alterations in structure and connectivity that are apparent in the neonatal period persist through early childhood into adulthood (Fischi-Gomez et al., 2014; Nosarti et al., 2014; Pandit et al., 2014). Brain structure and IQ are strongly heritable (Thompson et al., 2001; Toga and Thompson, 2005), and the incorporation of geometric information about tracts has proven useful for studying heritability of brain integrity and connectivity inferred from dMRI in adults (Jin et al., 2011). We propose that *R* may offer a new tool for studying genetic contributions to brain structure in the newborn, which to date has been investigated using FA and morphometry but has not included shape analysis of major fasciculi (Boardman et al., 2014).

Tract-averaged values of ⟨D⟩ were higher and FA values were lower in all eight TOIs in preterm infants at term equivalent age compared with controls in bivariate analysis. After adjustment for PMA at scan, which was necessary because both metrics change rapidly during perinatal brain development (Huppi et al., 1998), ⟨D⟩ was only increased in genu and splenium, while FA was reduced in the splenium and left ILF. Our findings are in broad agreement with previous region-of-interest (Counsell et al., 2006; Huppi et al., 1998; McKinstry et al., 2002; Rose et al., 2007; Skiold et al., 2010), voxel-based (Gimenez et al., 2008; Thompson et al., 2014), and tractography approaches (Aeby et al., 2009; Anjari et al., 2007; Thompson et al., 2011), which show that preterm infants at term equivalent age have higher ⟨D⟩ and lower FA in white matter compared with term controls, although the anatomic localization of these changes is inconsistent between studies and the role of confounding morbidities is uncertain.

The relationship between water diffusion biomarkers and white matter development is complex because the maturational processes of axonal fasciculation, pre-myelination (proliferation of glial cell bodies, extension of oligodendroglial processes, increase in macromolecules and membrane density), and true myelination (ensheathment of axons) are all anisotropic (Beaulieu, 2002; Nossin-Manor et al., 2013; Zanin et al., 2011), and the sequence of these processes is not uniform across neural systems. Therefore, while dMRI biomarkers provide sensitive measures of tissue microstructure, they are also non-specific. We found that tracts were separable based on water diffusion parameters, with the greatest difference observed between CST, CCG and splenium.

Fig. 1. Mean reference tract calculated from the control training data displayed in green and overlaid on the age-specific standard space template. The tracts displayed are genu (a, axial) and splenium (b, axial) of corpus callosum, left CCG (c, sagittal), right CCG (d, sagittal), left CST (e, coronal), right CST (f, coronal), left ILF (g, sagittal), and right ILF (h, sagittal).

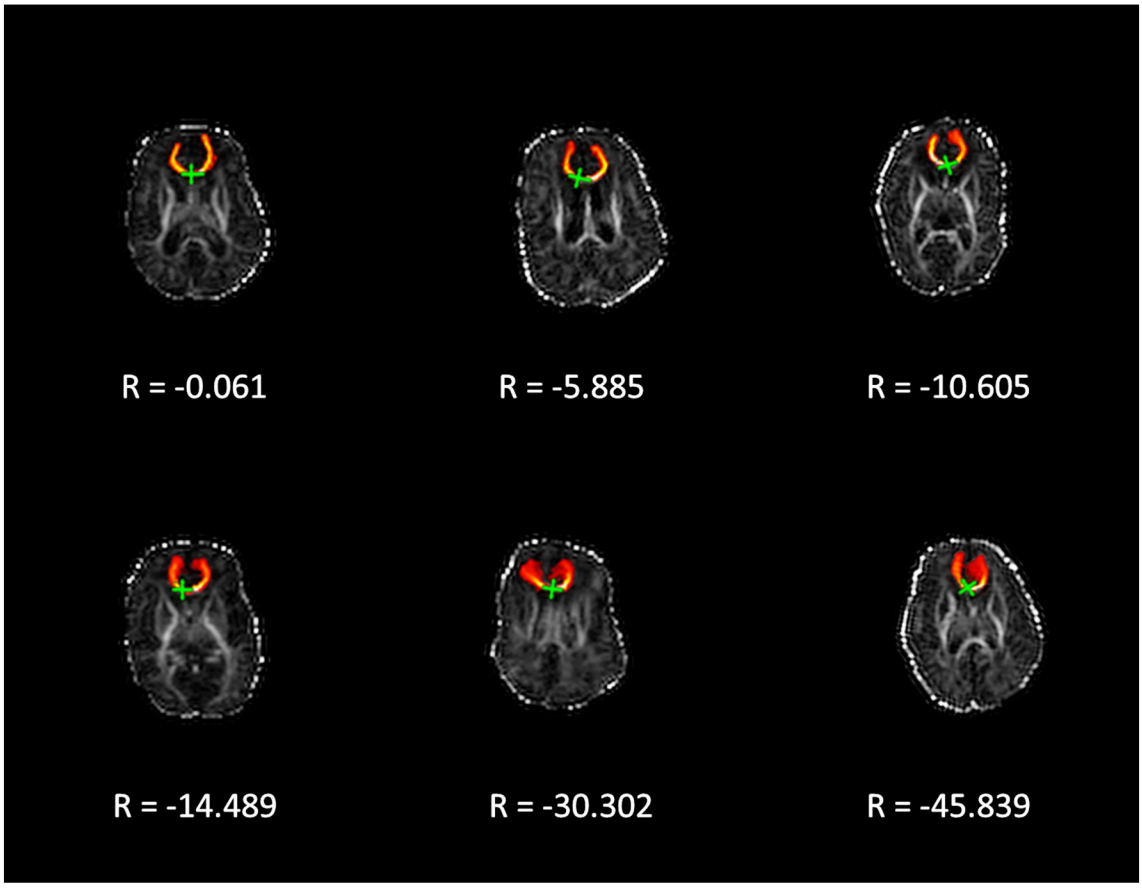

Fig. 2. Illustration of the range of absolute goodness-of-fit values (R) observed in the preterm group for genu of the corpus callosum overlaid on FA maps. As values of *R* become increasingly negative, the deviation of tract topology from reference topology (Fig. 1a) increases.

This suggests that adult patterning of neural systems (Bastin et al., 2010) is present very early in development, and before the onset of widespread myelination.

Systematic review of 5 randomized controlled trials shows that antenatal $MgSO_4$ reduces the burden of cerebral palsy and other motor impairments in the offspring of women who deliver very preterm (Doyle et al., 2007), but there is some doubt about long term benefit and none of the studies were designed to assess function in other domains as a primary outcome (Chollat et al., 2014; Doyle et al., 2014). Magnesium is thought to act on a number of cellular targets and processes in preterm brain injury, which are not restricted to motor systems, so it is plausible that tissue effects might be apparent in other neural systems. We found a modest but significant reduction in ⟨D⟩ in the splenium of preterm infants who had been exposed to antenatal $MgSO_4$ compared with untreated infants, after adjustment for relevant confounders. The splenium connects parietal, temporal and visual cortices, so these data indicate that antenatal $MgSO_4$ exposure has beneficial tissue effects that extend beyond motor systems. Detailed evaluation across all developmental domains of infants exposed to antenatal $MgSO_4$ is needed to understand fully its treatment effects. Finally, our data suggest that tract-averaged water diffusion parameters may provide useful biomarkers to complement voxel-wise approaches (such as Tract-based Spatial Statistics) for evaluating neuroprotective strategies in the newborn (O'Gorman et al., 2015; Porter et al., 2010).

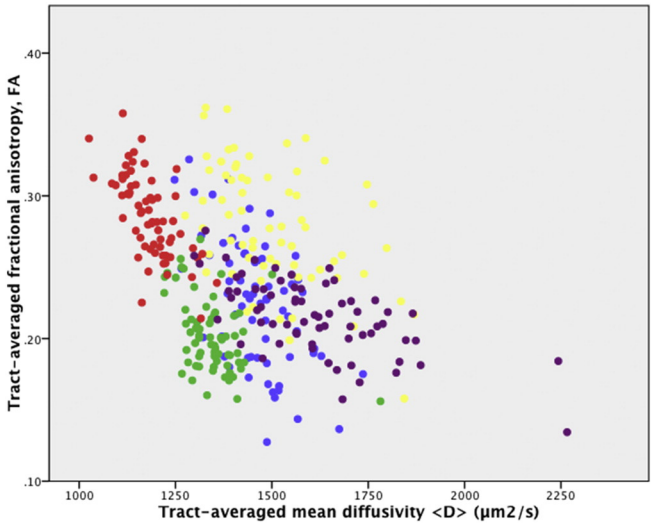

Fig. 3. Scatterplot of tract-averaged FA against tract-averaged ⟨D⟩ in all segmented tracts for every participant: genu (dark blue); splenium (yellow); CST (red); CCG (green); ILF (purple).

PNT has some limitations in neonates. First, we were unable to identify uncinate and arcuate fasciculi in the training set although these tracts can be segmented from adult data using PNT (Clayden et al., 2007); this is likely due to lower resolution inherent to neonatal dMRI or relative under-development of these tracts at term equivalent age. Second, the success of PNT varied from 100% for CST to 82% for right CCG in the preterm group, which may be explained by differential susceptibility to partial volume effects for different tracts. A further potential limitation relates to multiple testing: eight simultaneous tests were carried out for the ⟨D⟩ and FA data respectively. Bonferroni correction is inappropriate here because tract-averaged FA and ⟨D⟩ values are

correlated across the brain (Penke et al., 2010), so we chose to control the effects of multiple testing with FDR at a threshold of 0.05. Finally, the choice of reference template is a potential source of bias: we chose a reference based on healthy controls born at term because it provided the most biologically 'normal' reference. Further work would be required to determine whether a reference template drawn from a representative sample of the entire study group influences the results.

5. Conclusions

We have shown that PNT, an automated single seed point tractography method, segments TOIs with a high degree of accuracy in the newborn brain. It is unique in providing information about tract topology, and it enables calculation of tract-averaged dMRI biomarkers. Tract topology is a marker of preterm birth that is relatively robust to age at scan. We found that discrete neural systems can be separated by water diffusion parameters, reflecting specific microstructural properties of tracts that are apparent in early life, and that tract-averaged dMRI biomarkers provide a sensitive metric for evaluating risk factors for preterm brain injury and neuroprotective treatment effects. The approach may have utility for investigating early life determinants of long-term neurologic and psychiatric disorders.

Conflicts of interest

The supporting sources had no role in study design or collection, analysis and interpretation of data, or writing of the report. None of the authors report biomedical financial interests or potential conflicts of interest.

Acknowledgements

The study was funded by Theirworld (http://www.theirworld.org), with the exception of a subset of four term controls that were acquired with funding from a Wellcome Trust Institutional Strategic Support Fund award (PI Jane E Norman, University Of Edinburgh). The study was supported by NHS, Research, Scotland and NHS Lothian, Research and Development. We are grateful to the families who consented to take part in the study and to the nursing and radiography staff at the Clinical Research Imaging Centre, University of Edinburgh (http://www.cric.ed.ac.uk) who participated in scanning the infants. We thank Thorsten Feiweier at Siemens for collaborating with dMRI acquisitions (Works-in-Progress Package for Advanced EPI Diffusion Imaging).

References

Aeby, A., Liu, Y., De Tiège, X., Denolin, V., David, P., Balériaux, D., Kavec, M., Metens, T., Van Bogaert, P., 2009. Maturation of thalamic radiations between 34 and 41 weeks' gestation: a combined voxel-based study and probabilistic tractography with diffusion tensor imaging. A.J.N.R. Am. J. Neuroradiol. 30 (9), 1780–1786. http://dx.doi.org/10.3174/ajnr.A1660195744497.

Anjari, M., Srinivasan, L., Allsop, J.M., Hajnal, J.V., Rutherford, M.A., Edwards, A.D., Counsell, S.J., 2007. Diffusion tensor imaging with tract-based spatial statistics reveals local white matter abnormalities in preterm infants. Neuroimage 35 (3), 1021–1027. http://dx.doi.org/10.1016/j.neuroimage.2007.01.03517344066.

Ball, G., Boardman, J.P., Aljabar, P., Pandit, A., Arichi, T., Merchant, N., Rueckert, D., Edwards, A.D., Counsell, S.J., 2013. The influence of preterm birth on the developing thalamocortical connectome. Cortex 49 (6), 1711–1721. http://dx.doi.org/10.1016/j.cortex.2012.07.00622959979.

Basser, P.J., Pajevic, S., Pierpaoli, C., Duda, J., Aldroubi, A., 2000. In vivo fiber tractography using DT-MRI data. Magn. Reson. Med. 44 (4), 625–632. http://dx.doi.org/10.1002/1522-2594(200010)44:4<625::AID-MRM17>3.0.CO;2-O11025519.

Bastin, M.E., Muñoz Maniega, S., Ferguson, K.J., Brown, L.J., Wardlaw, J.M., MacLullich, A.M., Clayden, J.D., 2010. Quantifying the effects of normal ageing on white matter structure using unsupervised tract shape modelling. Neuroimage 51 (1), 1–10. http://dx.doi.org/10.1016/j.neuroimage.2010.02.03620171285.

Bastin, M.E., Pettit, L.D., Bak, T.H., Gillingwater, T.H., Smith, C., Abrahams, S., 2013. Quantitative tractography and tract shape modeling in amyotrophic lateral sclerosis. J. Magn. Reson. Imaging 38 (5), 1140–1145. http://dx.doi.org/10.1002/jmri.2407323450730.

Beaulieu, C., 2002. The basis of anisotropic water diffusion in the nervous system — a technical review. N.M.R. Biomed. 15 (7–8), 435–455. http://dx.doi.org/10.1002/nbm.78212489094.

Behrens, T.E., Berg, H.J., Jbabdi, S., Rushworth, M.F., Woolrich, M.W., 2007. Probabilistic diffusion tractography with multiple fibre orientations: what can we gain? Neuroimage 34 (1), 144–155. http://dx.doi.org/10.1016/j.neuroimage.2006.09.01817070705.

Behrens, T.E., Johansen-Berg, H., Woolrich, M.W., Smith, S.M., Wheeler-Kingshott, C.A., Boulby, P.A., Barker, G.J., Sillery, E.L., Sheehan, K., Ciccarelli, O., Thompson, A.J., Brady, J.M., Matthews, P.M., 2003. Non-invasive mapping of connections between human thalamus and cortex using diffusion imaging. Nat. Neurosci. 6 (7), 750–757. http://dx.doi.org/10.1038/nn107512808459.

Bhutta, A.T., Cleves, M.A., Casey, P.H., Cradock, M.M., Anand, K.J., 2002. Cognitive and behavioral outcomes of school-aged children who were born preterm: a meta-analysis. JAMA 288 (6), 728–737. http://dx.doi.org/10.1001/jama.288.6.72812169077.

Blencowe, H., Cousens, S., Chou, D., Oestergaard, M., Say, L., Moller, A.B., Kinney, M., Lawn, J., Born Too Soon Preterm Birth Action Group, 2013. Born too soon: the global epidemiology of 15 million preterm births. Reprod. Health 10 (Suppl. 1), S2. http://dx.doi.org/10.1186/1742-4755-10-S1-S224625129.

Boardman, J.P., Counsell, S.J., Rueckert, D., Kapellou, O., Bhatia, K.K., Aljabar, P., Hajnal, J., Allsop, J.M., Rutherford, M.A., Edwards, A.D., 2006. Abnormal deep grey matter development following preterm birth detected using deformation-based morphometry. Neuroimage 32 (1), 70–78. http://dx.doi.org/10.1016/j.neuroimage.2006.03.02916675269.

Boardman, J.P., Walley, A., Ball, G., Takousis, P., Krishnan, M.L., Hughes-Carre, L., Aljabar, P., Serag, A., King, C., Merchant, N., Srinivasan, L., Froguel, P., Hajnal, J., Rueckert, D., Counsell, S., Edwards, A.D., 2014. Common genetic variants and risk of brain injury after preterm birth. Pediatrics 133 (6). http://dx.doi.org/10.1542/peds.2013-301124819575.

Chollat, C., Enser, M., Houivet, E., Provost, D., Bénichou, J., Marpeau, L., Marret, S., 2014. School-age outcomes following a randomized controlled trial of magnesium sulfate for neuroprotection of preterm infants. J. Pediatr. 165 (2), 398–400. http://dx.doi.org/10.1016/j.jpeds.2014.04.00724837863.

Clark, C.A., Woodward, L.J., Horwood, L.J., Moor, S., 2008. Development of emotional and behavioral regulation in children born extremely preterm and very preterm: biological and social influences. Child Dev. 79 (5), 1444–1462. http://dx.doi.org/10.1111/j.1467-8624.2008.01198.x18826535.

Clayden, J.D., Bastin, M.E., Storkey, A.J., 2006. Improved segmentation reproducibility in group tractography using a quantitative tract similarity measure. Neuroimage 33 (2), 482–492. http://dx.doi.org/10.1016/j.neuroimage.2006.07.01616956774.

Clayden, J.D., Jentschke, S., Muñoz, M., Cooper, J.M., Chadwick, M.J., Banks, T., Clark, C.A., Vargha-Khadem, F., 2012. Normative development of White matter tracts: similarities and differences in relation to age, gender, and intelligence. Cereb. Cortex 22 (8), 1738–1747. http://dx.doi.org/10.1093/cercor/bhr24321940703.

Clayden, J.D., Muñoz Maniega, S., Storkey, A.J., King, M.D., Bastin, M.E., Clark, C.A., 2011. TractoR: magnetic resonance imaging and tractography with R. J. Stat. Softw. 44 (8), 1–18.

Clayden, J.D., Storkey, A.J., Bastin, M.E., 2007. A probabilistic model-based approach to consistent white matter tract segmentation. I. E.E.E. Trans. Med. Imaging 26 (11), 1555–1561. http://dx.doi.org/10.1109/TMI.2007.90582618041270.

Conturo, T.E., Lori, N.F., Cull, T.S., Akbudak, E., Snyder, A.Z., Shimony, J.S., McKinstry, R.C., Burton, H., Raichle, M.E., 1999. Tracking neuronal fiber pathways in the living human brain. Proc. Natl. Acad. Sci. U S A 96 (18), 10422–10427. http://dx.doi.org/10.1073/pnas.96.18.1042210468624.

Counsell, S.J., Shen, Y., Boardman, J.P., Larkman, D.J., Kapellou, O., Ward, P., Allsop, J.M., Cowan, F.M., Hajnal, J.V., Edwards, A.D., Rutherford, M.A., 2006. Axial and radial diffusivity in preterm infants who have diffuse white matter changes on magnetic resonance imaging at term-equivalent age. Pediatrics 117, 376–386. http://dx.doi.org/10.1542/peds.2005-082016452356.

Crump, C., Winkleby, M.A., Sundquist, K., Sundquist, J., 2010. Preterm birth and psychiatric medication prescription in young adulthood: a Swedish national cohort study. Int. J. Epidemiol. 39 (6), 1522–1530. http://dx.doi.org/10.1093/ije/dyq10320570995.

Doyle, L.W., Anderson, P.J., Haslam, R., Lee, K.J., Crowther, C., Australasian Collaborative Trial of Magnesium Sulphate (ACTOMgSO4) Study Group, 2014. School-age outcomes of very preterm infants after antenatal treatment with magnesium sulfate vs placebo. JAMA 312 (11), 1105–1113. http://dx.doi.org/10.1001/jama.2014.1118925226476.

Doyle, L.W., Crowther, C.A., Middleton, P., Marret, S., Rouse, D., 2007. Magnesium sulphate for women at risk of preterm birth for neuroprotection of the fetus. Cochrane Database Syst. Rev. CD004661.

Elgen, S.K., Leversen, K.T., Grundt, J.H., Hurum, J., Sundby, A.B., Elgen, I.B., Markestad, T., 2012. Mental health at 5 years among children born extremely preterm: a national population-based study. Eur. Child Adolesc. Psychiatry 21 (10), 583–589. http://dx.doi.org/10.1007/s00787-012-0298-122752364.

Fischi-Gómez, E., Vasung, L., Meskaldji, D.E., Lazeyras, F., Borradori-Tolsa, C., Hagmann, P., Barisnikov, K., Thiran, J.P., Hüppi, P.S., 2014. Structural brain connectivity in school-age preterm infants provides evidence for impaired networks relevant for higher order cognitive skills and social cognition. Cereb. Cortex http://dx.doi.org/10.1093/cercor/bhu07324794920.

Giménez, M., Miranda, M.J., Born, A.P., Nagy, Z., Rostrup, E., Jernigan, T.L., 2008. Accelerated cerebral white matter development in preterm infants: a voxel-based morphometry study with diffusion tensor MR imaging. Neuroimage 41 (3), 728–734. http://dx.doi.org/10.1016/j.neuroimage.2008.02.02918430590.

Halmøy, A., Klungsøyr, K., Skjærven, R., Haavik, J., 2012. Pre- and perinatal risk factors in adults with attention-deficit/hyperactivity disorder. Biol. Psychiatry 71 (5), 474–481. http://dx.doi.org/10.1016/j.biopsych.2011.11.01322200325.

Hüppi, P.S., Maier, S.E., Peled, S., Zientara, G.P., Barnes, P.D., Jolesz, F.A., Volpe, J.J., 1998. Microstructural development of human newborn cerebral white matter assessed in vivo by diffusion tensor magnetic resonance imaging. Pediatr. Res. 44 (4), 584–590. http://dx.doi.org/10.1203/00006450-199810000-000199773850.

Jin, Y., Shi, Y., Joshi, S.H., Jahanshad, N., Zhan, L., de Zubicaray, G.I., McMahon, K.L., Martin, N.G., Wright, M.J., Toga, A.W., Thompson, P.M., 2011. Heritability of white matter fiber tract shapes: a HARDI study of 198 twins. Multimodal Brain Image Anal (2011) 2011, 35–43. http://dx.doi.org/10.1007/978-3-642-24446-9_525346947.

Johnson, S., Hollis, C., Kochhar, P., Hennessy, E., Wolke, D., Marlow, N., 2010. Psychiatric disorders in extremely preterm children: longitudinal finding at age 11 years in the EPICure study. J. Am. Acad. Child Adolesc. Psychiatry 49 (5), 453–463. http://dx.doi.org/10.1016/j.jaac.2010.02.00220431465.

Kerr-Wilson, C.O., Mackay, D.F., Smith, G.C., Pell, J.P., 2012. Meta-analysis of the association between preterm delivery and intelligence. J. Public Health (Oxf) 34 (2), 209–216. http://dx.doi.org/10.1093/pubmed/fdr02421393308.

Kuklisova-Murgasova, M., Aljabar, P., Srinivasan, L., Counsell, S.J., Doria, V., Serag, A., Gousias, I.S., Boardman, J.P., Rutherford, M.A., Edwards, A.D., Hajnal, J.V., Rueckert, D., 2011. A dynamic 4D probabilistic atlas of the developing brain. Neuroimage 54 (4), 2750–2763. http://dx.doi.org/10.1016/j.neuroimage.2010.10.01920969966.

McKinstry, R.C., Miller, J.H., Snyder, A.Z., Mathur, A., Schefft, G.L., Almli, C.R., Shimony, J.S., Shiran, S.I., Neil, J.J., 2002. A prospective, longitudinal diffusion tensor imaging study of brain injury in newborns. Neurology 59 (6), 824–833. http://dx.doi.org/10.1212/WNL.59.6.82412297561.

Moore, T., Hennessy, E.M., Myles, J., Johnson, S.J., Draper, E.S., Costeloe, K.L., Marlow, N., 2012. Neurological and developmental outcome in extremely preterm children born in England in 1995 and 2006: the EPICure studies. BMJ 345, e7961. http://dx.doi.org/10.1136/bmj.e796123212880.

Moster, D., Lie, R.T., Markestad, T., 2008. Long-term medical and social consequences of preterm birth. N. Engl. J. Med. 359 (3), 262–273. http://dx.doi.org/10.1056/NEJMoa070647518635431.

Nosarti, C., Nam, K.W., Walshe, M., Murray, R.M., Cuddy, M., Rifkin, L., Allin, M.P., 2014. Preterm birth and structural brain alterations in early adulthood. Neuroimage Clin. 6, 180–191. http://dx.doi.org/10.1016/j.nicl.2014.08.00525379430.

Nosarti, C., Reichenberg, A., Murray, R.M., Cnattingius, S., Lambe, M.P., Yin, L., MacCabe, J., Rifkin, L., Hultman, C.M., 2012. Preterm birth and psychiatric disorders in young adult life. Arch. Gen. Psychiatry 69 (6), E1–E8. http://dx.doi.org/10.1001/archgenpsychiatry.2011.137422660967.

Nossin-Manor, R., Card, D., Morris, D., Noormohamed, S., Shroff, M.M., Whyte, H.E., Taylor, M.J., Sled, J.G., 2013. Quantitative MRI in the very preterm brain: assessing tissue organization and myelination using magnetization transfer, diffusion tensor and T imaging. Neuroimage 64, 505–516. http://dx.doi.org/10.1016/j.neuroimage.2012.08.08622982360.

O'Gorman, R.L., Bucher, H.U., Held, U., Koller, B.M., Hüppi, P.S., Hagmann, C.F., Swiss EPO Neuroprotection Trial Group, 2015. Tract-based spatial statistics to assess the neuroprotective effect of early erythropoietin on white matter development in preterm infants. Brain 138 (2), 388–397. http://dx.doi.org/10.1093/brain/awu36325534356.

Pandit, A.S., Robinson, E., Aljabar, P., Ball, G., Gousias, I.S., Wang, Z., Hajnal, J.V., Rueckert, D., Counsell, S.J., Montana, G., Edwards, A.D., 2014. Whole-brain mapping of structural connectivity in infants reveals altered connection strength associated with growth and preterm birth. Cereb. Cortex 24, 2324–2333. http://dx.doi.org/10.1093/cercor/bht08623547135.

Penke, L., Muñoz Maniega, S., Murray, C., Gow, A.J., Hernández, M.C., Clayden, J.D., Starr, J.M., Wardlaw, J.M., Bastin, M.E., Deary, I.J., 2010. A general factor of brain white matter integrity predicts information processing speed in healthy older people. J. Neurosci. 30 (22), 7569–7574. http://dx.doi.org/10.1523/JNEUROSCI.1553-10.201020519531.

Porter, E.J., Counsell, S.J., Edwards, A.D., Allsop, J., Azzopardi, D., 2010. Tract-based spatial statistics of magnetic resonance images to assess disease and treatment effects in perinatal asphyxial encephalopathy. Pediatr. Res. 68 (3), 205–209. http://dx.doi.org/10.1203/PDR.0b013e3181e9f1ba20520585.

Rose, J., Mirmiran, M., Butler, E.E., Lin, C.Y., Barnes, P.D., Kermoian, R., Stevenson, D.K., 2007. Neonatal microstructural development of the internal capsule on diffusion tensor imaging correlates with severity of gait and motor deficits. Dev. Med. Child Neurol. 49 (10), 745–750. http://dx.doi.org/10.1111/j.1469-8749.2007.00745.x17880643.

Serag, A., Aljabar, P., Ball, G., Counsell, S.J., Boardman, J.P., Rutherford, M.A., Edwards, A.D., Hajnal, J.V., Rueckert, D., 2012. Construction of a consistent high-definition spatio-temporal atlas of the developing brain using adaptive kernel regression. Neuroimage 59 (3), 2255–2265. http://dx.doi.org/10.1016/j.neuroimage.2011.09.06221985910.

Skiöld, B., Horsch, S., Hallberg, B., Engström, M., Nagy, Z., Mosskin, M., Blennow, M., Adén, U., 2010. White matter changes in extremely preterm infants, a population-based diffusion tensor imaging study. Acta Paediatr. 99 (6), 842–849. http://dx.doi.org/10.1111/j.1651-2227.2009.01634.x20132144.

Thompson, D.K., Inder, T.E., Faggian, N., Johnston, L., Warfield, S.K., Anderson, P.J., Doyle, L.W., Egan, G.F., 2011. Characterization of the corpus callosum in very preterm and full-term infants utilizing MRI. Neuroimage 55 (2), 479–490. http://dx.doi.org/10.1016/j.neuroimage.2010.12.02521168519.

Thompson, D.K., Lee, K.J., Egan, G.F., Warfield, S.K., Doyle, L.W., Anderson, P.J., Inder, T.E., 2014. Regional white matter microstructure in very preterm infants: predictors and 7 year outcomes. Cortex 52, 60–74. http://dx.doi.org/10.1016/j.cortex.2013.11.01024405815.

Thompson, P.M., Cannon, T.D., Narr, K.L., van Erp, T., Poutanen, V.P., Huttunen, M., Lönnqvist, J., Standertskjöld-Nordenstam, C.G., Kaprio, J., Khaledy, M., Dail, R., Zoumalan, C.I., Toga, A.W., 2001. Genetic influences on brain structure. Nat. Neurosci. 4 (12), 1253–1258. http://dx.doi.org/10.1038/nn75811694885.

Toga, A.W., Thompson, P.M., 2005. Genetics of brain structure and intelligence. Annu. Rev. Neurosci. 28, 1–23. http://dx.doi.org/10.1146/annurev.neuro.28.061604.13565515651931.

Woodward, L.J., Anderson, P.J., Austin, N.C., Howard, K., Inder, T.E., 2006. Neonatal MRI to predict neurodevelopmental outcomes in preterm infants. N. Engl. J. Med. 355 (7), 685–694. http://dx.doi.org/10.1056/NEJMoa05379216914704.

Zanin, E., Ranjeva, J.P., Confort-Gouny, S., Guye, M., Denis, D., Cozzone, P.J., Girard, N., 2011. White matter maturation of normal human fetal brain. An in vivo diffusion tensor tractography study. Brain Behav. 1 (2), 95–108. http://dx.doi.org/10.1002/brb3.1722399089.